Electro-Oxidation of Ethanol on Pt, Rh, and PtRh Electrodes. A Study Using DEMS and in-Situ FTIR Techniques

J. P. I. de Souza,[†] S. L. Queiroz, K. Bergamaski, E. R. Gonzalez, and F. C. Nart*

Instituto de Química de São Carlos, Universidade de São Paulo, C.P. 780, 13560-970 São Carlos (SP), Brazil

Received: December 31, 2001; In Final Form: May 12, 2002

The electrochemical oxidation of ethanol on platinum, rhodium, and platinum−rhodium electrodes is studied using on-line differential electrochemical mass spectrometry (DEMS) and in-situ infrared spectroscopy (FTIR). The data were normalized using the oxidation of a CO monolayer in order to compare the activity of the different electrodes. Three products have been detected, namely CO_2 and acetaldehyde (detected by DEMS) and acetic acid (detected by in-situ FTIR, since acetic acid is not volatile enough to be detected by DEMS). It is found that rhodium is the far less active electrocatalyst for ethanol electrochemical oxidation. Pure platinum and $Pt_{90}Rh_{10}$ present similar overall normalized current density, but $Pt_{90}Rh_{10}$ presents a better CO_2 yield than pure platinum. The best CO_2 yield is found for the $Pt_{73}Rh_{27}$ electrodes. The acetaldehyde yield decreases as rhodium is added to the electrode. The ratio CO_2/CH_3CH_2O increases when rhodium is added to the electrode. The possible reasons for the different reactivity for the studied electrodes is discussed in terms of C−H bond activation and C−O bond coupling on the different surfaces.

Introduction

The development of fuel cells operating directly with liquid organic fuels has increased the interest on the electrochemical oxidation of alcohols and other small organic molecules.[1−7] Wang et al.,[5] using on-line mass spectrometry under fuel cell operating conditions, have shown that ethanol can be a promising alternative for direct methanol fuel cells.

Platinum electrocatalysts are well-known to be active for the electrochemical oxidation of organic molecules in acid media. However, adsorbed CO resulting from the reaction poisons the electrode and drastically reduces the activity of pure platinum. To improve the electrocatalytic activity of platinum, addition of a second element has been widely used to form a bimetallic catalyst. Examples of these materials are PtRu,[6−8] PtSn,[8−10] PtMo,[11] etc. The bimetallic electrodes composed of PtRu are known to be significantly effective for methanol and ethanol oxidation.[12,13] Particularly, PtRu bimetallic electrodes represent a very promising alternative for the direct methanol fuel cell. However, other bimetallic electrodes, such as PtRh electrocatalysts, can also show high activity and were not so widely investigated. PtRh electrodes have been used in a methanol oxidation study,[14] but, at least to our knowledege, no investigations have been carried out on ethanol oxidation using such electrodes. Although not related to the electrochemical oxidation reactions, it is interesting to note that supported PtRh catalysts (commonly known as three-way catalysts) are largely employed in the exhaust system of automotive engines for NO_x reduction and CO oxidation.[15]

Supported PtRh bimetallic electrodes were used in the past for molecular H_2 oxidation as a CO-tolerant electrodes.[16] It was also found that the addition of 24 at. % Rh presented the best activity for CO-contaminated H_2 fuel and that the enhanced activity was not due to tolerance to CO, but to an intrinsic higher catalytic activity of the alloy, related to the excess of unpaired electrons per atom in the alloy, compared to pure platinum.

The modified electronic structure of a bimetallic catalyst may also play a role in the electrocatalysis of ethanol oxidation. Therefore, it is the aim of the present work to examine the influence of PtRh electrode composition on the electrocatalytic activity toward the electrochemical oxidation of ethanol using differential electrochemical mass spectrometry (DEMS) and in-situ Fourier transform IR spectroscopy (FTIRS). These techniques are used in order to follow directly the formation of the reaction products during the applied potential programs.

Experimental Section

The electrodes were obtained by potentiostatic deposition of Pt or Rh or co-deposition of Pt and Rh onto either a smooth (polished to a mirror finishing) gold disk of 0.38 cm^2 geometric area for the FTIR measurements, or on a sputtered gold layer (1.13 cm^2 area, 50 nm thickness) on a PTFE membrane (SCIMAT thickness 60μm, mean pore size 0.17 μm, 50% porosity) for DEMS measurements. All electrodepositions were made for 5 min at 0.2 V vs RHE in a 1 M $HClO_4$ solution containing the appropriate amount of Pt and Rh salts.

The atomic bulk compositions of the electrodeposited electrodes were determined by EDAX (energy dispersive analysis of X-rays).

The reference electrode was a reversible hydrogen electrode (RHE) in the electrolyte solution, and a platinized Pt foil was used as the auxiliary electrode.

Solutions were prepared with Millipore-MilliQ water and analytical grade $HClO_4$ acid (Merck), ethanol (99.5%, Merck), ethanal (99.5%, Merck), $H_2PtCl_6 \cdot 6H_2O$ (Aldrich), and $RhCl_3 \cdot 3H_2O$ (Aldrich). High purity CO and N_2 gases were used.

FTIR Measurements. FTIR spectra were obtained with a BOMEM DA-8 spectrometer equipped with a liquid nitrogen cooled MCT detector. A PTFE spectroelectrochemical cell coupled to a CaF_2 prismatic window was used. Each spectrum

* Corresponding author.
[†] On leave from the Universidade Federal do Pará, Departamento de Química, Rua Augusto Correa, s/n, Campus do Guamá, Belém, PA, Brazil.

10.1021/jp014645c CCC: $22.00
Published on Web 08/31/2002

TABLE 1: Normalization Factors Calculated from CO-Stripping Experiments (see text)

DEMS			FTIR	
electrodes (EDAX composition)	normalization factors for CVs (Q_{ox}/C)	normalization factors for MSCVs ($Q_m/10^{-11}$ C)	electrodes (EDAX composition)	normalization factors for integrated band intensities (in-situ FTIR)
Pt	0.0121	3.639	Pt	1.289
Rh	0.0263	5.586	Rh	3.750
$Pt_{90}Rh_{10}$	0.0205	11.106	$Pt_{90}Rh_{10}$	4.007
$Pt_{73}Rh_{27}$	0.0359	18.323	$Pt_{76}Rh_{24}$	2.213
$Pt_{55}Rh_{45}$	0.0274	16.911	$Pt_{64}Rh_{36}$	4.426

corresponds to 256 interferometer scans taken at 8 cm^{-1} resolution at different potentials in the range 0.35−1.1 V for ethanol oxidation reaction. The spectra are presented in the form of the reflectance ratio R/R_o of a single beam spectrum R obtained at a given potential and a reference spectrum R_o obtained at 0.05 or 0.3 V, for ethanol. Only p-polarized light was used.

DEMS Measurements. A computer-controlled quadrupole mass spectrometer, MKS Instruments, was used for the DEMS measurements. Details on this method were given elsewhere.[17,18] Briefly, the method allows the on-line detection of volatile and gaseous products of electrochemical reactions during the application of a potential scan. The electrochemical cell was constructed according to the principles described elsewhere.[19]

In a typical DEMS experiment the current vs potential curves (cyclic voltammograms (CVs)) are recorded simultaneously with the mass intensity vs potential curves (mass spectrometric cyclic voltammograms (MSCVs)), for selected values of m/z (mass/charge) ion signals. The potential was cycled in the range 0.05−1.1 V and the scan rate was 0.01 V s^{-1}.

Normalization Procedure. To compare the intrinsic activities of different catalysts it is indispensable to normalize their response with respect to the number of active surface sites. A normalization method for the signals obtained from cyclic voltammetry (electrochemical currents), DEMS (mass/charge intensities), and FTIR techniques (integrated band intensities) was presented in a previous paper.[20] Briefly, the oxidative stripping of a saturated CO monolayer was used to calculate the normalization factors for each of the measured parameters. For this purpose the CO saturation coverage on the catalyst was achieved by bubbling CO for 5 min at 0.2 V followed by bubbling N_2 for 10 min in order to eliminate dissolved CO.

For the voltammetric currents of cyclic voltammograms the normalization factor is the charge Q_{ox} necessary to oxidize a CO monolayer. For the mass spectrometry signals it is the integrated corresponding signal (Q_m) for the CO_2 ($m/z = 44$) produced during CO stripping. For the FTIR spectra it is the integrated band intensity for the CO-saturated catalyst. The values of the normalization factors are listed in Table 1.

Results

DEMS Study. DEMS was used to follow only the formation of the volatile reaction products: CO_2 and acetaldehyde. Acetic acid that has been detected as a third product in ethanol oxidation cannot be detected in low concentrations due to its low volatility and because weak acids are more strongly ionized in dilute solution. Acetaldehyde can be followed by the mass signal $m/z = 29$ corresponding to the fragment $[CHO]^+$. The mass signal for $m/z = 44$ is the main peak of true CO_2 fragmentation, corresponding to $[CO_2]^{+\cdot}$. However, the acetaldehyde molecular species $[CH_3CHO]^+$ also contributes to the $m/z = 44$ mass signal. To estimate the true CO_2 production, the ion current for

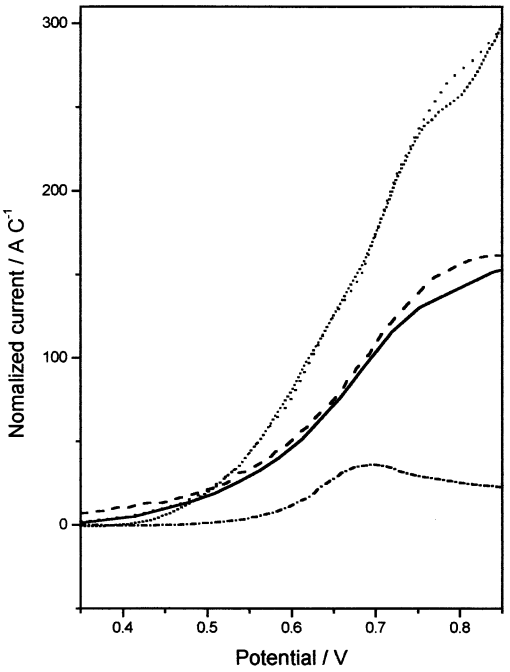

Figure 1. Anodic normalized scans of voltammograms (CVs) in 0.1 M EtOH + 0.1 M $HClO_4$. Scan rate 10 mV s^{-1}. (·····) Pt; (· · ·) $Rt_{90}Rh_{10}$; (—) $Pt_{73}Rh_{27}$; (- - -) $Pt_{55}Rh_{45}$; (—·—) Rh.

$m/z = 44$ has to be corrected by subtracting the contribution of the interfering fragment of acetaldehyde. This can be achieved through the experimental determination of the relative intensity of the $[CH_3CHO]^+$ fragment ($m/z = 44$) with respect to the main acetaldehyde peak $[CHO]^+$ ($m/z = 29$) using pure acetaldehyde. The value obtained under the present experimental conditions[21] was 17.4%. Hence, from the $m/z = 44$ mass intensity signal was subtracted 17.4% of the $m/z = 29$ mass intensity signal to obtain a *corrected* $m/z = 44$ signal (related only to CO_2 production).

The normalized CVs obtained in 0.1 M EtOH + 0.1 M $HClO_4$ are shown in Figure 1. The normalized electric currents due to ethanol oxidation on the different electrode compositions show a very similar electrocatalytic activity between Pt and $Pt_{90}Rh_{10}$ electrodes and, with lower currents, between $Pt_{73}Rh_{27}$ and $Pt_{55}Rh_{45}$ electrodes. Rh has the worst response.

Since in fuel cell applications it is desirable to fully oxidize the fuel, it is important to check for the best electrocatalytic activity for CO_2 production. The corresponding normalized mass signals for CO_2 (corrected $m/z = 44$) are presented in Figure 2 and show that the activity of the bimetallic PtRh electrodes compared to pure platinum electrodes depends on the electrode composition. The $Pt_{73}Rh_{27}$ electrode has the highest activity for potentials up to 0.8 V. The $Pt_{55}Rh_{45}$ electrode has a slightly higher activity than Pt until 0.7 V, while $Pt_{90}Rh_{10}$ and pure rhodium present an electrocatalytic activity poorer than the pure platinum electrode. From these results an approximate order of activities for CO_2 production, in the range 0.4−0.7 V, can be established: $Pt_{73}Rh_{27} > Pt_{55}Rh_{45} > Pt > Pt_{90}Rh_{10} \cong Rh$.

The onset of CO_2 mass signal, related to the catalytic activity of the material, also changes with the electrode composition. On a $Pt_{73}Rh_{27}$ electrode the onset for CO_2 production is displaced about 0.05 V to less positive potentials in relation to the pure platinum electrode.

The comparison of the activity for acetaldehyde production shows a completely different behavior, as can be seen in Figure 3. The pure platinum electrode presents the highest mass signal intensity, in agreement with the fact that the highest electro-

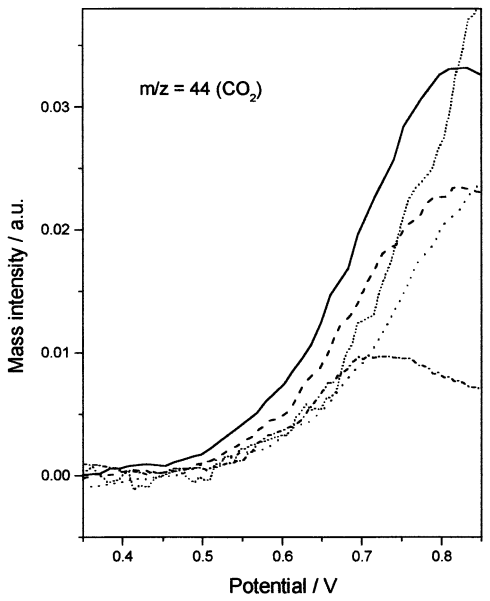

Figure 2. Normalized mass intensities for corrected $m/z = 44$ (corrected CO_2 signal, see text). (·····)Pt; (· · ·) $Rt_{90}Rh_{10}$; (—) $Pt_{73}Rh_{27}$; (- - -) $Pt_{55}Rh_{45}$; (—·—) Rh.

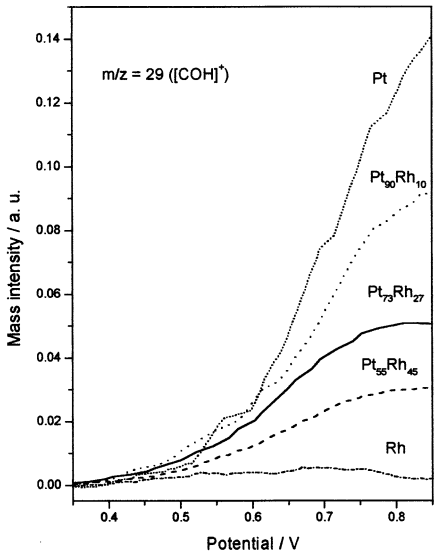

Figure 3. Normalized mass intensities for m/z = 29 (acetaldehyde signal). (·····) Pt; (· · ·) $Rt_{90}Rh_{10}$; (—) $Pt_{73}Rh_{27}$; (- - -) $Pt_{55}Rh_{45}$; (—·—) Rh.

chemical current is observed for the pure platinum electrode. For the bimetallic electrodes the mass signal intensity for acetaldehyde production decreases as the amount of rhodium increases in the alloy. The onset of acetaldehyde production as observed in Figure 3 is ca. 0.4 V and does not depend on the electrode.

The ratio between the $m/z = 44$ and the $m/z = 29$ signals can give a clue on the effect of rhodium on the relative selectivity toward CO_2 production. These results do not represent an absolute measure of the selectivity, since the $m/z = 29$ signal is not an absolute measure of the total acetaldehyde production. Clearly the ratio of the $m/z = 44$ over the $m/z = 29$ signals increases from pure platinum to pure rhodium electrodes (see Table 2), showing that the addition of rhodium to platinum increases the complete oxidation of ethanol to CO_2. Total ethanol oxidation entails both C−H and C−C bond dissociation

TABLE 2: DEMS Signal Ratio of the ($m/z = 44$)/($m/z = 29$) for the Different Electrode Compositions

electrode	$(m/z = 44)/(m/z = 29)$ $E = 0.7$ V
Pt	0.17
$Pt_{90}Rh_{10}$	0.17
$Pt_{73}Rh_{27}$	0.49
$Pt_{55}Rh_{45}$	0.67
Rh	1.8

followed by CO−O bond coupling. Thus, a better activity for total ethanol oxidation does not mean a better electrode catalytic activity, since pure platinum and the $Pt_{90}Rh_{10}$ electrodes present the highest electric currents, meaning that the turnover frequency is governed by the partial oxidation. Indeed, the mass signal intensity for the $m/z = 29$ fragment is much higher than the mass signal intensity $m/z = 44$ for CO_2 in all electrodes.

In-Situ FTIR Study. The vibrational bands associated with ethanol electro-oxidation products, CO_2, acetic acid, and acetaldehyde, on smooth Pt electrodes have already been assigned.[22] The band at 2344 cm^{-1} is due to CO_2 formation. The bands at 1277, 1391, and 1715 cm^{-1} indicate acetic acid production. The main acetaldehyde bands are located at 1113, 1352, and 1713 cm^{-1}. Unfortunately, the acetaldehyde bands overlap with acetic acid and perchlorate ions (1100 cm^{-1}) bands.

Two sets of spectra in 0.1 M EtOH + 0.1 M $HClO_4$ solution for electrodeposited Pt and on $Pt_{90}Rh_{10}$ electrodes are shown in Figure 4, parts a and b, respectively. It is possible to observe the development of the CO_2 band in both sets of spectra. However, the band at 1274 cm^{-1}, due to acetic acid, is clearly seen to start at 0.9 V and slightly increases with the increase of the potential for the Pt electrode (Figure 4a) while for the PtRh electrode no features characteristic of acetic acid or acetaldehyde formation could be detected. It important to point out that the strong upward band (centered at 1643 cm^{-1}, Figure 4) due to water leaving the thin layer cavity can overlap the carbonyl band (1715 cm^{-1}) of the acetaldehyde. The same spectral features presented for the $Pt_{90}Rh_{10}$ electrode composition were also found with the other PtRh electrode compositions and for electrodeposited Rh, that is, CO_2 was the only detected product. Tacconi et al.[23] reported similar FTIR results for a smooth Rh electrode, using the same ethanol concentration as in this work.

To rationalize the different results for the different techniques, that is the detection of acetaldehyde by DEMS and not by in-situ FTIR, it is assumed that the procedure used for the in-situ FTIR experiments allows the further oxidation of the partially oxidized products. Indeed, carbon dioxide produced at each potential in the in-situ FTIR experiment is trapped in the cavity of the thin layer, thus producing an accumulation effect on spectra taken in a sequence of potential steps as in the present case. On the contrary, DEMS is an on-line experiment, the products are continually pumped away quickly, preventing further oxidation.

Another source of discrepancies between DEMS and FTIR results can be related to a difference in electrode surface properties. Ethanol oxidation to form CO_2 is actually a very complex reaction involving adsorption steps, which are known to be highly dependent on the structure of the surface.[24−26] Considering that the DEMS and FTIR electrodeposited electrodes have different textures (see Experimental Section), due to the different Au substrates used in the preparation, some differences in the nature and in the number of surface defects can play a role in the overall ethanol electro-oxidation reaction.

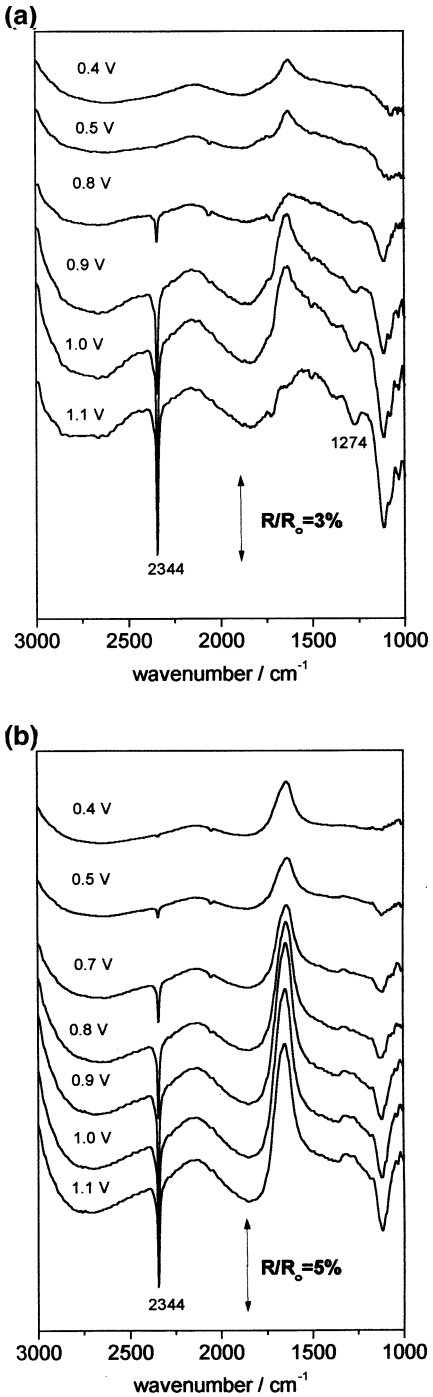

Figure 4. Two collections of spectra during ethanol oxidation on (a) electrodeposited Pt and (b) electrodeposited $Pt_{90}Rh_{10}$. 0.1 M EtOH + 0.1 M $HClO_4$, 256 scans, 8 cm^{-1} resolution.

Discussion

The composition of the bimetallic electrode given in this study is the bulk composition and not the surface composition. Bimetallic phases may have different bulk and surface compositions. Differences in surface and bulk composition are caused by surface segregation of one component. It has been recognized that the driving force to surface segregation is the difference in the enthalpy of sublimation of the two elements. Pt and Rh have very close enthalpy of vaporization and surface segregation should not occur for this alloy, but experimentally surface segregation with platinum enrichment has been found when the alloy is submitted to temperatures above 1000 K.[27] However, no segregation has been found when the crystal was submitted to 700 K. This temperature-dependent segregation was assigned to a vibrational entropy effect.[28] Indeed, Langeveld and Niemanstsverdriet[28] show that including the vibrational entropy term they could reproduce the surface segregation of platinum at 1000 K. In another study, Legrand and Tréglia,[29] using the tight-biding Ising model (TBIM) showed that the temperature-dependent segregation could be explained by an energy- and not entropy-dependent term (the entropic term is negligible in the TBIM model). Independent of the divergences in interpretation, it is clear that segregation in PtRh alloys is expected to be very small at room temperatures.

A complication that can arise is the segregation induced by electrochemical electrode activation by oxidation−reduction cycles. In the present case we used always a freshly prepared surface and did not polarize the electrode at potentials higher than 1.0 V to avoid surface oxidation. Another possibility would be adsorbate-induced surface segregation. In this case the reaction intermediates could induce surface segregation, mainly OH adsorbates which are needed to accomplish the full oxidation. However, we are not aware of data on possible adsorbate-induced surface segregation for PtRh alloys. Even for the well studied PtRu alloy electrodes[4,6,30−32] there is only data for surface composition before the reaction and no information on reaction-induced surface segregation is known so far.

Another factor that could affect the electrode composition and likely also the surface composition is the texture of the electrodes. Indeed, using the same solutions for the PtRh electrodeposition there are deviations of the bulk composition as detected by EDAX when the smooth or porous gold was used (see Table 1). This effect is more pronounced for higher rhodium content. However, it is interesting to point out that no significant differences in surface segregation at defects on PtRh alloys have been detected for samples annealed up to 1000 K.[27] Therefore we believe that, although the bulk composition can differ in electrodeposits due to the differences in the electrode texture, surface segregation should not be strongly affected by the different textures of the electrode.

A remarkable result of this study is the observation that the addition of rhodium to platinum electrodes improves the selectivity toward complete electrochemical oxidation of ethanol to CO_2. At the same time, a pure rhodium electrode presents the lowest reaction rate. The best bimetallic electrode presents an overall reaction rate (or turnover frequency), as measured by the total normalized current, of the same order of the pure platinum electrode, the worst CO_2/acetaldehyde ratio. In fact, in a previous study Tacconi et al.[23] identified that the major product for smooth polycrystalline rhodium electrodes is CO_2, but the results were not compared with those for pure platinum or bimetallic electrodes.

However, the increased activity for C−C bond dissociation is not followed by a higher overall reaction rate, as can be seen from the much lower normalized current for the pure rhodium electrode compared to pure platinum. There are many possible reasons for the slower reaction rate of ethanol electrochemical oxidation on rhodium electrodes.

The first possibility is that pure rhodium electrodes are much less efficient than platinum for the dehydrogenation reaction. A very high barrier to dehydrogenation can hinder the C−C bond dissociation to form CO, thus causing a slower overall reaction rate. The reaction to produce acetaldehyde is a typical reaction involving only the abstraction of one hydrogen per molecule by the surface. Indeed, analyzing the normalized mass signal intensity for acetaldehyde ($m/z = 29$) it is clear that the acetaldehyde yield decreases from pure platinum to rhodium

in a continuous way. This is an indication that the hydrogen capture by the surface decreases as rhodium is added to platinum. Therefore the CO coverage during the reaction must be lower on rhodium and rhodium-containing surfaces. Unfortunately rough surfaces are not appropriate to acquire quantitative data for adsorbed species, since there are many optical artifacts that hinder the acquisition of confident data.[33]

Although for pure rhodium a slower dehydrogenation reaction can be the reason for the lower overall reaction rate, this does not seem to be the case for the $Pt_{73}Rh_{27}$ bimetallic electrode, where the normalized mass signal intensity for CO_2 is higher than that for the pure platinum electrode.

Another possible reason for the slower reaction rate can be related to the apparently strong CO−Rh bonding, as revealed by the difficulty of totally removing a CO monolayer from a Rh(111) electrode.[34] It is found that more than 20 voltammetric cycles are required to oxidize the adsorbed CO monolayer in order to recover the clean Rh(111) surface. This result is in agreement with the values obtained for the CO bonding energy in gas-phase conditions. The bonding energy for CO adsorbed on polycrystalline platinum is 25 kJ mol^{-1}, while for CO adsorbed on polycrystalline rhodium is 134 kJ mol^{-1}.[35] Probably a larger difference must be expected in the electrochemical environment. To our knowledge, no direct data of bonding energy in the electrochemical environment are available. Alternatively, the stronger oxygen−rhodium bonding (293 kJ mol^{-1})[36] compared to platinum−oxygen (≈167 kJ mol^{-1})[37] may be the reason of the difficulty for the electrochemical oxidation of CO on rhodium. The strong O−Rh bond energy may produce a high activation energy for the CO−O coupling hindering the CO oxidation reaction. A direct consequence is the lower oxidation rate, associated with an increased poisoning of the surface by adsorbed CO. Unfortunately, we are not aware of data for the activation energy for the CO oxidation on Pt and Rh electrodes. The activation energy for $CO_{ads} + O_{ads} \rightarrow CO_{2(gas)}$ on a polycrystalline Pt foil has been reported to be 100 kJ mol^{-1}, while for the same reaction on a polycrystalline Rh foil is 105 kJ mol^{-1}.[35] This is a quite small difference to account for the large difference in the reaction rate observed for the electrochemical reaction. It is likely that the difference in activation energy is larger for the electrode reaction. In the electrochemical environment there are other components that can alter the adsorption energy of CO and O and therefore the activation energy for the CO and O coupling.

In a qualitative analysis, the shift in the onset for CO_2 production to lower overpotentials for the bimetallic $Pt_{75}Rh_{25}$ clearly shows that the activation energy for the CO + O reaction is lower than on pure platinum and pure rhodium. No such effect was observed for the acetaldehyde production.

The same reaction on PtRu bimetallic electrodes shows that the onset potential for the CO_2 production is decreased from 0.6 V for pure platinum to 0.38 V for $Pt_{92}Ru_8$ at 25 °C[7] in a 1 M ethanol solution, or from 0.5 to 0.25 V in a 0.1 M ethanol solution.[38] This is a remarkable decrease of more than 0.2 V when compared to a decrease of ca. 0.05 V for the best PtRh bimetallic electrode. On PtRu bimetallic electrodes it has been observed also a decrease in the onset potential for acetaldehyde production.

A contrasting result for PtRu bimetallic electrodes, compared to PtRh bimetallic electrodes, is the acetalhdehyde/CO_2 ratio. On PtRu bimetallic electrodes the addition of Ru does not improve the production of CO_2 over acetaldehyde production, as observed here for the PtRh bimetallic electrodes. Thus, addition of rhodium clearly increases the ability for C−C bond dissociation, which is not observed for the PtRu electrocatalysts. On the other hand, Ru really produces a significant decrease for the onset potential for the overall reaction.

The reason for the differences observed for PtRh and PtRu bimetallic electrodes rely on the possible different action of the second element. It has been largely accepted that on PtRu electrodes predominates the so-called bifunctional mechanism, where the platinum sites act to dehydrogenate the molecule and to accommodate the adsorbed CO, while the ruthenium sites act to provide the necessary oxygen at lower potentials than platinum, thus causing a decrease in the onset potential for CO oxidation. Curiously, on bimetallic PtRu alloys also the C−H bond activation seems to be affected by the presence of ruthenium, as attested by a decrease in the onset potential for acetaldehyde production.[35,36] On the other hand, the role of rhodium on bimetallic PtRh electrodes, seems to be related to a more intrinsic electrocatalytic property and not as a site to promote more readily the oxygen necessary for the CO oxidation. Working with bimetallic PtRh electrodes as CO tolerant electrodes for H_2 oxidation, Ross et al.[16] conclude that the enhancement of the reaction rate by adding rhodium to the electrode is not due to a CO tolerant effect, but to an increase of the catalytic activity associated to the changes in the electronic properties caused by the addition of rhodium to platinum.

All these results suggest that for ethanol oxidation the presence of rhodium in the electrode composition seems to be important to improve the C−C bond dissociation, but it is not enough to produce a good electrocatalyst, since rhodium does not help in decreasing significantly the barrier for the CO oxidation. On the other hand, addition of ruthenium helps in decreasing the energy for CO−O coupling and possibly also the activation energy for the dehydrogenation process. Possibly, a good electrocatalyst for this reaction needs the presence of rhodium and ruthenium to improve both the dehydrogenation process, the C−C bond dissociation, and the CO−O coupling. Such study is under way in our laboratory.

Conclusion

The combination of platinum and rhodium in bimetallic electrodes for ethanol oxidation shows that rhodium produces a strong decrease in the acetaldehyde yield, compared to pure platinum electrodes. The CO_2 yield is improved relative to pure platinum on $Pt_{73}Rh_{27}$ and $Pt_{55}Rh_{45}$, the best being the $Pt_{73}Rh_{27}$ composition. Although the selectivity for CO_2 over acetaldehyde production increases, only the $Pt_{90}Rh_{10}$ presents an overall reaction current similar to that of a platinum electrode. However, the increase in the selectivity toward CO_2 formation over acetaldehyde shows that PtRh bimetallic electrodes are promising candidates for ethanol oxidation if a third element is added to improve the overall reaction rate. Probably ruthenium is a good candidate to add to the electrocatalyst to supply sites to form more active oxygen and to improve the CO−O bond coupling to increase the rate of CO_2 production.

Acknowledgment. The authors thank the CAPES, CNPq, and FAPESP Brazilian agencies for the financial support and Prof. Vielstich for the valuable discussions.

References and Notes

(1) Beden, B.; Lamy, C.; Léger, J.-M. In *Modern Aspects of Electrochemistry*; Bockris, J. O., Conway, B. E., White, R. E., Eds.; Plenum: New York, 1992; Vol. 22.

(2) Parsons, R.; Vandernoot, T. *J. Electroanal. Chem*. **1988**, *257*, 9.

(3) Iwasita, T.; Vielstich, W. In *Advances in Electrochemical Sciences and Engineering*; Gerischer, H., Tobias, C. W., Eds.; VCH: Weinheim, 1990; Vol. 1.

(4) Gasteiger, H. A.; Markovic, N.; Ross, P. N., Jr.; Cairns, E. J. *Electrochim. Acta* **1994**, *39*, 1825.

(5) Wang, J.; Wasmus, S.; Savinell, R. F. *J. Electrochem. Soc.* **1995**, *142*, 4218.

(6) Gasteiger, H. A.; Markovic, N.; Ross, P. N., Jr.; Cairns, E. J. *J. Phys. Chem*. **1993**, *97*, 12020.

(7) Schmidt, V. M.; Ianniello, R.; Pastor, E.; Gonzáles, S. *J. Phys. Chem.* **1996**, *100*, 17901.

(8) Morimoto, Y.; Yeager, E. B. *J. Electroanal. Chem.* **1998**, *444*, 95.

(9) Hable, C. T.; Wrighton, M. S. *Langmuir* **1993**, *9*, 3284.

(10) Frelink, T.; Visscher, W.; Van Veen, J. A. R. *Surf. Sci.* **1995**, *335*, 353.

(11) Kita, H.; Nakajima, H.; Shimazu, K. *J. Electroanal. Chem.* **1988**, *248*, 181.

(12) Souza, J. P. I.; Rabelo, J. F. B.; Moraes, I. R.; Nart, F. C. *J. Electroanal. Chem.* **1997**, *420*, 17.

(13) Iwasita, T.; Nart, F. C.; Vielstich, W. *Ber. Bunsen-Ges. Phys. Chem.* **1990**, *94*, 1030.

(14) Koch, D. F. A.; Rand, D. A. J.; Woods, R. *J. Electroanal. Chem.* **1976**, *70*, 73.

(15) Sasahara, A.; Tamura, H.; Tanaka, K.-I. *J. Phys. Chem. B* **1997**, *101*, 1186.

(16) Ross, P. N.; Kinoshita, K.; Scarpellino, A. J.; Stonehardt, P. *J. Electroanal. Chem*. **1975**, *59*, 177.

(17) Bittins-Cattaneo, B.; Cattaneo, E.; Königshoven, P.; Vielstich, W. In *Electroanalytical Chemistry—A Series of Advances*; Bard, A. J., Ed.; Marcel Dekker: New York, 1991; Vol. 17.

(18) Wolter, O.; Heitbaum, J. *Ber. Bunsen-Ges. Phys. Chem***. 1984**, *88*, 6.

(19) Ianniello, R.; Schmidt, V. M. Ber. *Bunsen-Ges. Phys. Chem*. **1995**, *99*, 83.

(20) Souza, J. P. I.; Iwasita, T.; Nart, F. C.; Vielstich, W. *J. Appl. Electrochem*. **1999**, *30*, 43.

(21) The fragmentation in the presence of water vapor is quite different from the pure gas phase. For the gas-phase fragmentation of acetaldehyde the $m/z = 44$ corresponds to 82% of the $m/z = 29$, while in the presence of water vapor under our experimental conditions to only 17.4%.

(22) Iwasita, T.; Rasch, B.; Cattaneo, E.; Vielstich, W. *Electrochim. Acta* **1989**, *34*, 1073.

(23) Tacconi, N. R.; Lezna, R. O.; Beden, B.; Lamy, C. *J. Electroanal. Chem.* **1994**, *379*, 329.

(24) Xia, X.; Liess, H.-D.; Iwasita, T. *J. Electroanal. Chem*. **1997**, *437*, 233.

(25) Shin, J.; Tornquist, J.; Korzeniewski, C.; Hoaglund, C. S. *Surf. Sci.* **1996**, *364*, 122.

(26) Schmiemann, U.; Müller, U.; Baltruschat, H. *Electrochim. Acta* **1995**, *40*, 99.

(27) Ren, D.; Tsong, T. T. *Surf. Sci.* **1987**, *184*, L439.

(28) van Langeveld, A. D.; Niemandtsverdriet, J. W. *J. Vac. Sci. Technol. A* **1987**, *5*, 558.

(29) Legrand, B.; Tréglia, G. *Surf. Sci.* **1990**, *236*, 398.

(30) Gasteiger, H. A.; Ross, P. N.; Cairns, E. J. *Surf. Sci*. **1993**, *293*, 67.

(31) Gasteiger, H. A.; Markovic, N.; Ross, P. N.; Cairns, E. J. *J. Phys. Chem.* **1994**, *98*, 617.

(32) Richarz, F.; Wohlmann, B.; Vogel, U.; Hoffschulz, H.; Wandelt, K. *Surf. Sci*. **1995**, *335*, 361.

(33) Park, S.; Tong, Y.; Wieckowski, A.; Weaver, M. J. *Electrochem. Commun.* **2001**, *3*, 509.

(34) Gómez, R.; Orts, J. M.; Feliu, J. M.; Clavilier, J.; Klein, L. H. *J. Electroanal. Chem*. **1997,** *432*, 1.

(35) Aum Mallen, M. P.; Schmidt, L. D. *J. Catal*. **1996**, *161*, 230.

(36) Root, T. W.; Schmidt, L. D.; Fisher, G. B. *Surf. Sci*. **1983**, *134*, 30.

(37) Campbell, C. T.; Ertl, G.; Kuipers, H.; Segner, J. *Surf. Sci*. **1981**, *107*, 220.

(38) Fukiwara, N.; Friedrich, K. A.; Stimming, U. *J. Electroanal. Chem.* **1999**, *472*, 120.